Short-Range Molecular Interactions Governing the Orientational Ordering of Apolar Molecules Dissolved in Nematic Solvents

Giorgio Celebre* and Giuseppina De Luca

Dipartimento di Chimica, Università della Calabria, I-87036 Rende (CS), Italy

Received: September 6, 2002; In Final Form: November 14, 2002

The present study of the ordering of apolar molecules dissolved in uniaxial mesophases has been carried out by a model where the interactions between the solute and the local medium are described on a molecular scale. On the contrary, the mutual interactions between the solvent molecules are not explicitly taken into account, but a mean description of the macroscopic anisotropy of the bulk of the solvent is provided. This is done by defining a "virtual" mesophase director whose instantaneous orientation in the solute molecular frame is randomly given step-by-step during the numerical calculation of the solute order parameters. This model has been applied to apolar molecules biphenylene, 1,4-dicyanobenzene, 1,4-dinitrobenzene, and *p*-benzoquinone. The predicted order parameters have been compared with the ^{1}H NMR experimental data obtained for the same compounds dissolved in nematic solvents EBBA and ZLI1132 and in the 55 wt % ZLI1132 + EBBA magic mixture, where long-range effects are believed to be very small. A nearly perfect matching of the simulated solute-ordering matrices with the data in the magic mixture has been found, thus strengthening the common assumption that long-range effects can be neglected in that mixture. The model has also been tested on so-called magic solutes cyclohexane, 1,4-*trans*-dimethylcyclocyclohexane, and *trans*-decalin (whose electronic structure should preclude significant anisotropic long-range interactions) dissolved in ZLI2452. Once more, we obtained excellent results in reproducing the experimental order parameters (Terzis, A. F.; Poon, C.-D.; Samulski, E. T.; Luz, Z.; Poupko, R.; Zimmermann, H.; Muller, K.; Toriumi, H.; Photinos, D. J. *J. Am. Chem. Soc.* **1996**, *118*, 2226) over a very large range of temperatures, and this is a further evidence of the validity of the approach.

Introduction

Molecular interactions in condensed phases represent a fundamental topic in chemistry and physics. The interest they arouse is so high, both from a theoretical and an application point of view, that all of the techniques able to shed more light on this subject are to be considered worthy to be studied and applied. In the field of soft matter and complex fluids, a prominent position is occupied by liquid crystals, and the NMR spectroscopy of molecules dissolved in liquid crystalline solvents (typically, nematics) is undoubtedly a powerful tool to investigate them. Since the first work in this field (the ^{1}H NMR spectrum of benzene in nematic solution by Saupe and Englert[1]), this technique has indeed been recognized as a very appealing means to study intermolecular potentials because of the peculiarity of the solute in acting as an internal probe of the orientational forces present in the mesophase. The effects of the solute−solvent interactions are manifested in (a) the increased complexity of ^{1}H NMR spectra, which are strongly affected by dipolar couplings between the $^1/_2$ spin *i* and *j* nuclei[2]

$$\tilde{\mathbf{D}}_{ZZij} = \left[\frac{1}{2}(3\cos^2\alpha - 1)\right]\left[\frac{2}{3}\sum_{\zeta,\xi}\mathbf{S}_{\zeta\xi}\mathbf{D}_{\zeta\xi ij}\right] \qquad (1)$$

as well as in (b) the appearance of quadrupolar splittings[3] (characterizing the deuterium NMR spectra), which for axially symmetric C−D bonds are

$$\langle\nu_q^i\rangle = \nu_q^i\sum_{\zeta\xi}\mathbf{S}_{\zeta\xi}\cos\theta_\zeta^i\cos\theta_\xi^i \qquad (2)$$

In eq 1, α is the angle between the magnetic field, defining the *Z* direction in the laboratory frame, and the director of the mesophase, and $\mathbf{D}_{ij}$ is the geometry-dependent dipolar coupling tensor expressed in the the molecular frame; in eq 2, ν_q^i is the static quadrupole interaction constant for the *i*th deuteron and θ_ζ^i is the angle between the C−D^i bond and the ζ axis in the molecular frame. Finally, in eqs 1 and 2, **S** is the solute Saupe traceless ordering matrix whose generic element is

$$\mathbf{S}_{\zeta\xi} = \frac{1}{2}\langle 3\cos\vartheta_\zeta\cos\vartheta_\xi - \delta_{\zeta\xi}\rangle = \frac{\int(3\cos\vartheta_\zeta\cos\vartheta_\xi - \delta_{\zeta\xi})\exp\left[-\frac{U(\Omega)}{kT}\right]d\Omega}{2\int\exp\left[-\frac{U(\Omega)}{kT}\right]d\Omega} \qquad (3)$$

In eq 3, $\cos\vartheta_\zeta$ represents the direction cosine of the director with the ζ molecular axis, $\delta_{\zeta\xi}$ is the Kronecker delta function, Ω is the set of angles defining the director orientation in the molecular frame, and $U(\Omega)$ is the potential describing the orientational solute−solvent interactions. By analyzing and interpreting ^{1}H NMR and ^{2}H NMR spectra, it is then possible to obtain the encrypted information about orientational order, which is useful in formulating theories on intermolecular interactions.

A complete, general description of the orientational potential experienced by a generic solute (also a simple rigid molecule)

* Corresponding author. E-mail: giorgio.celebre@unical.it. Fax: (39)-0984492044. Phone: (39)0984492109.

10.1021/jp026923t CCC: $25.00
Published on Web 03/19/2003

in a generic nematic solvent is an arduous task because the entangled contributions due to short-ranged "size- and shape-" dependent repulsive forces and long-ranged electrostatic and dispersion forces must be taken into account. The importance of the two mechanisms is well documented in the literature,[3−7] but the relative weights of these influences are very hard to assess accurately;[8] nevertheless, the studied effects can be emphasized or minimized by a targeted choice of liquid crystal solvents and/or solutes, thus reducing the difficulty of the problem.

In the last few years, scientific effort has been mainly focused on the investigation of short-range mechanisms, which are nowadays generally recognized as the most important ones. As far as the solvents are concerned, to isolate the short-range effects on the solute ordering properly a particular "zero average electric field gradient" mixture (often called the magic mixture) has been created[9] by mixing in an appropriate ratio (depending on the solute and the temperature) of nematic solvents ZLI1132 (a Merck commercial eutectic mixture of alkylcyclohexylcyanobenzenes and alkylcyclohexylcyanobiphenyl) and EBBA (*N*-(4-ethoxybenzylidene)-4′-*n*-butylaniline). It has been observed by deuterium NMR that D_2 molecules dissolved in a 55 wt % ZLI1132 + 45 wt % EBBA mixture at 301.4 K do not feel the coupling between their electric quadrupole moment and the average electric field gradient of the solvent, commonly believed to be the main long-range orientational mechanism.[4] In principle, by changing the temperature and/or the solute, the composition of the mixture should also be varied to obtain strictly a zero-average electric field gradient on the probe molecules. Despite this apparently severe restriction, models based on purely short-range mechanisms are able to predict, for dilute solutions, the order parameters of several very different solutes in 55 wt % ZLI1132 + EBBA within just a 10% error.[4] The thinking that long-range effects can be quite safely neglected (in ordinary ranges of temperature and at low concentrations) for any kind of molecule dissolved in this mixture (in particular for apolar molecules[8]) is indeed becoming rather common, but it is worthwhile to emphasize that there is no proof of this and evidence regarding this matter is always to be sought.

Regarding the solutes, a class of compounds exists (the so-called magic solutes[4]) where short-range, repulsive intermolecular forces should be decisive in dictating the ordering. These molecules are indeed relatively inert, as are the cycloalkane solutes[3] whose electronic structure precludes significant anisotropic long-range electrostatic interactions.[4] The surviving long-range interaction should involve the polarizability, but this property seems to have a relatively negligible contribution to their order.[3]

With these premises, a sound and promising model based on short-range forces should be able in principle to predict well the experimental order parameters of small, apolar, rigid solutes (to simplify the problem) dissolved in the magic mixture and of magic solutes in a generic nematic solvent: the aim of this work is indeed the validation of a recently proposed short-range potential[10] that proved to be very effective in the past.[11] At the same time, the results of this paper could supply further proof of the "magic" nature of the 55 wt % ZLI1132 + EBBA mixture as a nematic solvent and of the cycloalkanes as solutes. Biaxial, apolar molecules biphenylene, 1,4-dicyanobenzene, 1,4-dinitrobenzene, and *p*-benzoquinone (the last three having strong local electric dipoles with which to test the possible effects of this property) in EBBA, ZLI1132, and the 55 wt % ZLI1132 + EBBA magic mixture have been considered. The solute-ordering matrices predicted by the model have been compared with those calculated from the dipolar couplings resulting from the analysis of ^{1}H NMR spectra of the probe molecules dissolved in the three nematics at different temperatures. The model has also been tested over a very large range of temperature on the following magic solutes: cyclohexane, 1,4-*trans*-dimethylcyclohexane, and *trans*-decalin, whose ^{2}H NMR measured experimental order parameters in ZLI2452 (a liquid crystal exhibiting a 120 °C nematic range, one of the widest existing) are available from the literature.[3]

The theoretical approach[10,11] that was used is delineated in the next section, followed by the experimental details of the work. In the subsequent section, the obtained results will be discussed, and finally, conclusions will be drawn.

Theoretical Background

There are basically two ways to face the orientational problem of a probe molecule dissolved in a liquid crystalline medium:

(A) the use of phenomenological molecular field models (where the solvent is generally described as a continuum);

B) the choice of simulation techniques (where the description of molecules is often oversimplified to make the problem easier to deal with).

In the A methodology, the shape and/or other properties of the solute are given in detail whereas, almost always, opportune solvent and temperature-dependent parameters, to which some kind of physical meaning is attributed, are optimized to obtain a good fitting of experimental data (see refs 7 and 8 for a general surveys of the existing models). The mean-field approaches are an effective tool to treat this complicated problem in a simple way, but they are not able to take into account specific interactions or other molecular effects that could be important (or determinant) in the description of the phenomenon.

In the B case, molecular interactions are explicitly given, but a direct comparison with experimental data is not strictly required since the aim of the simulations is to be paradigm of general physical behaviors. (See ref 10 for a wide selection of examples.) Unfortunately, simulation results are crucially dependent on system size.[12] As exhaustively explained in chapter 5 of ref 13a, if N particles are involved in the simulation and only short-range forces are taken into account, then the CPU time increases in principle as N^2 (although the use of the so-called neighbor lists can improve the efficiency up to $N \ln N$ or N, provided the code is written sensibly). So, when the physics of the studied problem (e. g., phase transitions) needs a large number of particles to be properly simulated, considerable (and not always available) computational resources are required. (However, far from the transition temperature, the system size requirements are not excessive, and meaningful molecular simulations can be carried out with very few solvent molecules in a very small periodic simulation box.)

In our opinion, the two philosophies, both having advantages and limitations, should not be seen as antithetical but rather as complementary. From this point of view, the model we propose[10,11] to describe a purely short-range anisotropic orientational potential could be considered to be a kind of "hybrid" between methods A and B outlined above. In this scheme, the solute particle, considered to be a collection of overlapping van der Waals spheres centered at the atomic positions, is crudely depicted after the manner of Straley[14] as embedded in a hard rectangular parallelepiped whose dimensions L, W, and B are defined by the projections of the molecular sizes along the **S** matrix principal axes. (It is worthwhile to stress that the similarities between our model and the Straley model are merely

limited to the representation of the particle as a rectangular block.) The solute molecule is located at the center of a cubic face-centered cage surrounded by six aspecific, prolate $D_{\infty h}$-symmetry solvent molecules (one for each face of the solute) characterized only by their orientations. This description is borrowed from previous lattice-model simulation studies[15] where, as usual in these kinds of approaches, translational degrees of freedom of solvent molecules are neglected. (Despite this seemingly paradoxical approximation, this choice seems to have no significant consequences on the prediction of short-range orientational order parameters; for more details, see ref 16, where practical advantages and conceptual disadvantages of lattice approaches are discussed.) From the lattice arrangement, the fact that each face of the solute is occupied by just one solvent molecule despite the different areas of the faces of the rectangular parallelepiped describing the solute is also derived. In our approach, the interactions of the solute with its direct uniaxial environment (the nearest-neighbor solvent molecules) are explicitly taken into account. On the contrary, the solvent−solvent molecular interactions are not considered explicitly: to avoid this complicated and CPU-time-consuming step, we instead resort to a mean description of the macroscopic anisotropy of the solvent by defining a "virtual" mesophase director produced by the self-organization of the other infinite solvent molecules far from the solute. The instantaneous orientation of the director in the solute molecular frame is given step-by-step during the numerical calculation of the solute order parameters. The basic idea of the model is that the anisotropic orienting potential experienced by the solute is the mean, over the six different faces of the parallelepiped representing the particle, of the tendency of each side of the box to align along the corresponding solvent molecule multiplied by the propensity of that solvent molecule to align to the director. The strictly short-range nature of this potential can be easily recognized since only the nearest solvent molecules directly interact with the solute and the interaction does not propagate beyond the distance of one molecule. Nonetheless, the information about the anisotropy of the bulk of the phase is not lost but it is transferred to the solute in an intermediate way via the nearest solvent molecules. Following this idea, the anisotropic solute(σ)−solvent(Σ) pair potential $U(\sigma, \Sigma)$ can be written as

$$\frac{U(\sigma, \sum)}{kT} = -\frac{\epsilon}{6}\sum_{h=1}^{6}\Lambda_h[P_2(\cos \psi_h^{\Lambda_h})P_2(\cos \omega_h)] \qquad (4)$$

where $\Lambda_h = W(\delta_{h1} + \delta_{h4}) + B(\delta_{h2} + \delta_{h5}) + L(\delta_{h3} + \delta_{h6})$, $P_2(\cos \theta)$ is the second Legendre polynomial; $\cos \psi_h^{\Lambda_h} = \vec{\mathbf{u}}_{\Lambda_h} \cdot \vec{\mathbf{k}}_h$, $\cos \omega_h = \vec{\mathbf{k}}_h \cdot \vec{\mathbf{n}}$, $\vec{\mathbf{u}}_{\Lambda_h}$ is the unit vector of the x, y, or z molecular frame axis along the $\Lambda_h \equiv L$, W, or B dimension of the solute; $\vec{\mathbf{k}}_h$ is the unit vector giving the instantaneous orientation of the hth solvent molecule in the molecular frame; and $\vec{\mathbf{n}}$ is the unit vector defining the direction of the virtual mesophase director in the molecular frame. The positive ϵ parameter, which has the dimension of inverse length, gives the intensity of the interactions: when an l-long segment is parallel to a solvent molecule aligned with the director, the orientational energy of the segment is $(E_l)/(kT) = \epsilon l$. (The minus sign in eq 4 favors parallel alignment.)

The averages giving the order parameters of the solute in the uniaxial mesophase (eq 3) cannot be calculated analytically when the potential reported in eq 4 is adopted, so they have been carried out by sampling with the help of random numbers. (In particular, the Monte Carlo−Metropolis sampling scheme[13b] has been used.) We proceeded, in a kind of "virtual experiment",

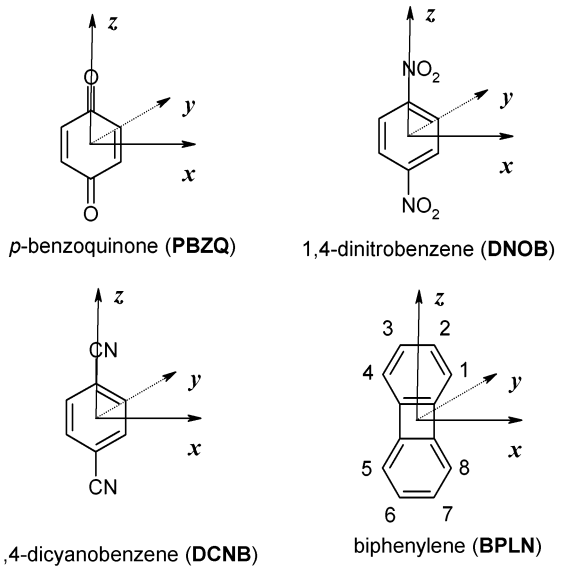

Figure 1. Structures and reference systems of solutes and proton numbering of biphenylene.

by varying the ϵ value (this is virtually equivalent to a sweep in temperature): for each different value of ϵ, 100 000 random orientations of the director $\vec{\mathbf{n}}$ in the solute frame have been generated. For each orientation (characterized by a (β, γ) couple of Euler angles), 10 000 non-mutually-interacting solute particles have been sampled, each of them surrounded by its randomly oriented sextet of solvent molecules. The number of orientation states of $\vec{\mathbf{n}}$ has been set on the basis of a mathematical argument to ensure a highly reliable convergence of the numerical multiple integration; on the contrary, the number of solute molecules has physical significance: it has been chosen to satisfy the required boundary conditions (a) $\mathbf{S}_{xx} = \mathbf{S}_{yy} = \mathbf{S}_{zz} = 0$ when $\epsilon = 0$ (isotropic condition) and (b) $\mathbf{S}_{xx} = \mathbf{S}_{yy} = \mathbf{S}_{zz} = 0$ when $L = W = B$ (lack of orientation of highly symmetric, i.e., cubic, particles). Calculations have been performed by using a very simple homemade code on a DIGITAL WorkStation series Alpha-600au equipped with a Digital Unix O.S.-V. 4.0; each run (corresponding to the calculations for a particular ϵ value) required only about 100 min of CPU time. (For more details about the simulation, see refs 10 and 11.)

Experimental Section

The four selected biaxial, apolar probe molecules *p*-benzoquinone (PBZQ), 1,4-dinitrobenzene (DNOB), 1,4-dicyanobenzene (DCNB), and biphenylene (BPLN) are shown in Figure 1 with the chosen molecular reference systems (where the **S** matrix is diagonal). The long molecular axes giving the lengths L of the molecules lie along z, the solute widths W are aligned with x, and the thicknesses B are parallel to y; in the same Figure, the proton numbering of BPLN is also given. The solutes are commercially available from Aldrich and were used without further purification. Very dilute solutions (∼1.5 mol %) were prepared dissolving each solute in nematic solvents ZLI1132 and EBBA and the 55 wt % ZLI1132 + EBBA mixture. (ZLI1132 was purchased from Merck Ltd., Darmstadt; EBBA was synthesized following standard procedures.[17]) Proton NMR spectra were recorded at different temperatures on a 7.04 T Bruker AC 300 spectrometer equipped with a temperature control unit. To obtain a good signal-to-noise ratio, the BPLN spectra were recorded with 32 scans compared to the usual 16 scans for the other solutes. The anisotropic spectra were analyzed, when possible, by the automated procedures based

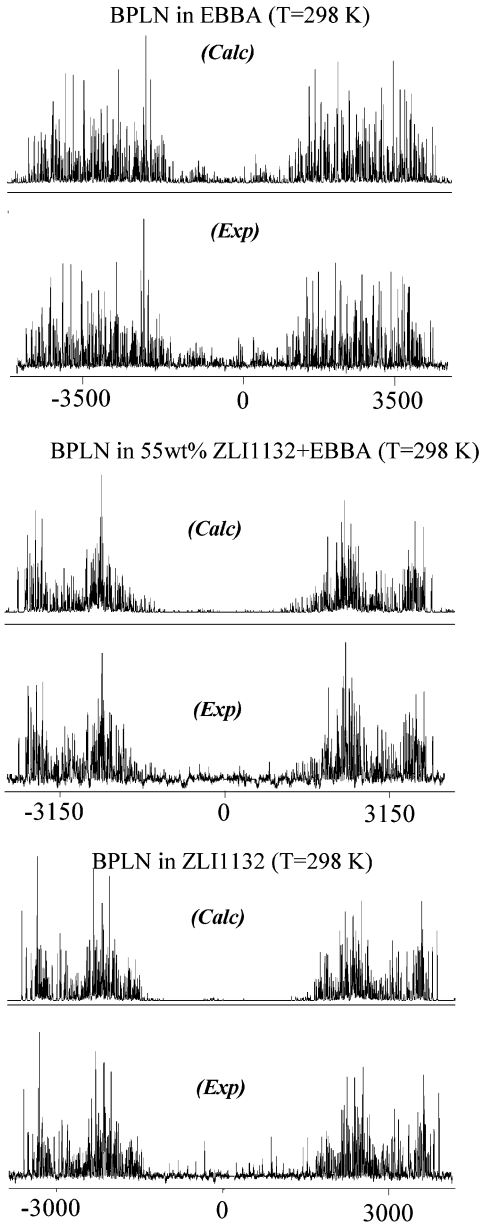

Figure 2. Experimental and calculated ^{1}H NMR spectra of biphenylene (BPLN) in the three different nematic solvents at room temperature.

on the work of Stephenson and Binsch[18] and developed by the University of Calabria NMR laboratory;[19] otherwise, graphical interactive strategies,[20] based on the Castellano and Bothner-By algorithm,[21] have been used. By way of example, the very complex room-temperature proton NMR spectra of partially oriented BPLN, for which, to our knowledge, only a multiple-quantum NMR study at 301.4 K in the magic mixture exists,[22] have been analyzed by assigning a total of 250 lines on about 500 experimental signals; once this had been done, the remaining lines, excluded from the fitting procedure either because they are overlapping lines or because they are weak, fell into place without trouble. In Figure 2 , the experimental spectra of BPLN in the three solvents, with their calculated counterparts, are shown.

The experimental dipolar couplings for the solutes are given in Tables 1−4.

Results and Discussion

Apolar Solutes in ZLI1132, EBBA, and the Magic Mixture. We used the model described in the theoretical section to calculate the order parameters at different temperatures of the solutes cited in the Experimental Section. The geometries adopted for BPLN, PBZQ, DCNB (point group of the mol-

TABLE 1: Experimental Dipolar Couplings from ^{1}H NMR Spectra of *p*-Benzoquinone Dissolved in Nematic Solvents ZLI1132 and EBBA and the 55 wt % ZLI1132 + EBBA Magic Mixture at Different Temperatures

ZLI1132			
T/K	D_{ortho}	D_{meta}	D_{para}
291	−1274.42 ± 0.10	−141.75 ± 0.11	−109.96 ± 0.11
296	−1245.44 ± 0.14	−134.17 ± 0.17	−105.16 ± 0.16
300	−1219.37 ± 0.35	−128.50 ± 0.48	−101.97 ± 0.52
305	−1182.07 ± 0.22	−120.66 ± 0.31	−96.73 ± 0.28
310	−1140.17 ± 0.28	−114.40 ± 0.33	−92.17 ± 0.33
315	−1088.36 ± 0.17	−106.88 ± 0.15	−86.57 ± 0.18
319	−1036.38 ± 0.23	−100.28 ± 0.22	−82.33 ± 0.22
323	−976.03 ± 0.48	−92.81 ± 0.54	−75.93 ± 0.55
55 wt % ZLI1132 + EBBA			
T/K	D_{ortho}	D_{meta}	D_{para}
294	−1624.24 ± 0.05	−20.21 ± 0.08	−60.69 ± 0.06
298	−1591.66 ± 0.07	−19.29 ± 0.07	−59.39 ± 0.07
303	−1535.38 ± 0.02	−18.24 ± 0.05	−56.97 ± 0.02
308	−1470.03 ± 0.22	−17.54 ± 0.29	−54.67 ± 0.25
313	−1400.63 ± 0.31	−16.27 ± 0.26	−52.42 ± 0.29
317	−1336.62 ± 0.18	−15.42 ± 0.42	−49.50 ± 0.19
321	−1267.77 ± 0.28	−14.58 ± 0.49	−47.10 ± 0.29
328	−1119.12 ± 0.19	−13.63 ± 0.21	−40.97 ± 0.22
EBBA			
T/K	D_{ortho}	D_{meta}	D_{para}
292	−2486.65 ± 0.09	132.53 ± 0.10	−12.46 ± 0.13
298	−2396.23 ± 0.30	125.08 ± 0.35	−13.19 ± 0.36
302	−2323.11 ± 0.02	119.97 ± 0.02	−13.33 ± 0.02
307	−2220.22 ± 0.28	112.23 ± 0.32	−13.10 ± 0.34
312	−2106.54 ± 0.36	104.49 ± 0.46	−14.50 ± 0.44
317	−1987.49 ± 0.27	95.52 ± 0.30	−14.32 ± 0.31
321	−1881.52 ± 0.25	89.38 ± 0.36	−15.84 ± 0.25

TABLE 2: Experimental Dipolar Couplings from ^{1}H NMR Spectra of 1,4-Dinitrobenzene Dissolved in Nematic Solvents ZLI1132 and EBBA and the 55 wt % ZLI1132 + EBBA Magic Mixture at Different Temperatures

ZLI1132			
T/K	D_{ortho}	D_{meta}	D_{para}
291	−2676.65 ± 0.34	58.07 ± 0.33	−59.79 ± 0.40
297	−2585.63 ± 0.28	50.25 ± 0.16	−61.73 ± 0.28
301	−2505.46 ± 0.12	44.79 ± 0.13	−60.80 ± 0.14
306	−2396.46 ± 0.21	37.63 ± 0.23	−61.02 ± 0.23
311	−2287.30 ± 0.30	23.90 ± 0.33	−62.07 ± 0.30
316	−2157.53 ± 0.10	25.83 ± 0.13	−60.21 ± 0.12
55 wt % ZLI1132 + EBBA			
T/K	D_{ortho}	D_{meta}	D_{para}
294	−2956.91 ± 0.12	144.51 ± 0.14	−28.82 ± 0.14
298	−2919.61 ± 0.02	141.91 ± 0.02	−28.69 ± 0.02
303	−2846.07 ± 0.08	136.58 ± 0.09	−28.78 ± 0.09
308	−2715.33 ± 0.19	126.94 ± 0.20	−29.75 ± 0.20
313	−2563.54 ± 0.26	116.57 ± 0.99	−28.73 ± 0.99
317	−2390.88 ± 0.70	105.82 ± 0.99	−30.63 ± 0.99
321	−2230.73 ± 0.74	94.47 ± 0.83	−28.39 ± 0.60
EBBA			
T/K	D_{ortho}	D_{meta}	D_{para}
292	−4470.87 ± 0.18	375.24 ± 0.19	32.91 ± 0.19
298	−4305.41 ± 0.23	356.02 ± 0.35	29.56 ± 0.37
302	−4180.27 ± 0.15	342.63 ± 0.16	26.81 ± 0.15
307	−3997.78 ± 0.16	323.31 ± 0.19	22.26 ± 0.17
312	−3798.49 ± 0.24	301.14 ± 0.21	20.26 ± 0.22
317	−3579.78 ± 0.31	279.73 ± 0.32	15.56 ± 0.32
321	−3390.77 ± 0.58	259.72 ± 0.62	12.73 ± 0.63

TABLE 3: Experimental Dipolar Couplings from ^{1}H NMR Spectra of 1,4-Dicyanobenzene Dissolved in Nematic Solvents ZLI1132 and EBBA and the 55 wt % ZLI1132 + EBBA Magic Mixture at Different Temperatures

ZLI1132			
T/K	D_{ortho}	D_{meta}	D_{para}
291	−4005.32 ± 0.19	282.42 ± 0.18	11.65 ± 0.19
297	−3873.87 ± 0.87	268.65 ± 0.22	9.17 ± 0.23
301	−3750.86 ± 0.24	256.47 ± 0.25	6.89 ± 0.25
306	−3582.58 ± 0.98	241.13 ± 1.38	2.47 ± 0.99
311	−3410.80 ± 0.52	223.80 ± 0.63	3.01 ± 0.87
55 wt % ZLI1132+EBBA			
T/K	D_{ortho}	D_{meta}	D_{para}
294	−3571.51 ± 0.30	262.66 ± 0.35	15.92 ± 0.35
298	−3490.37 ± 0.22	255.58 ± 0.26	15.29 ± 0.27
303	−3347.98 ± 0.08	243.51 ± 0.09	13.49 ± 0.09
308	−3182.98 ± 0.07	229.46 ± 0.08	11.76 ± 0.08
313	−3002.69 ± 0.27	214.36 ± 0.33	10.08 ± 0.33
317	−2844.50 ± 0.74	200.25 ± 0.73	12.97 ± 0.60
EBBA			
T/K	D_{ortho}	D_{meta}	D_{para}
292	−4352.23 ± 0.17	386.57 ± 0.19	53.21 ± 0.20
298	−4250.53 ± 0.12	377.13 ± 0.16	51.57 ± 0.15
302	−4124.61 ± 0.40	363.72 ± 0.42	49.70 ± 0.52
307	−3973.09 ± 0.25	351.08 ± 0.30	47.06 ± 0.27
312	−3781.55 ± 0.17	331.80 ± 0.20	43.89 ± 0.17
317	−3580.35 ± 0.37	312.59 ± 0.51	39.75 ± 0.54
321	−3402.89 ± 0.31	296.21 ± 0.50	38.14 ± 0.51

ecules: D_{2h}), and DNOB have been found in the literature,[22−25] as well as the van der Waals radii for the different atoms forming the studied solutes.[26−29] For DNOB, according to X-ray studies,[30,31] a rigid D_2 symmetry structure has been assumed, with both nitro groups twisted about the C−N bonds so that the NO_2 planes form angles of approximately 10.2° with the benzene ring plane. In this way, assuming an $\hat{ONO}$ angle of 124.28° [31] and a vdW radius of $r(O) = 1.52$ Å,[26] the nitro groups in the molecule do not emerge with respect to the ring thickness so that the B value of the molecule (3.40 Å) is essentially determined by the phenyl group. The resulting dimensions of the boxes embedding the solutes are reported in Table 5. In Figure 3, the solute orientational biaxialities $\mathbf{S}_{zz}-\mathbf{S}_{xx}$ of PBZQ, DNOB, DCNB, and BPLN (from the top to the bottom) as a function of $\mathbf{S}_{yy}$ are shown; the increasing direction of T is also indicated on the abscissas, and diagonal dashed lines on the plots separate the zones where the molecules are statistically oriented as rods from those where the orientational behavior can be assimilated to that of disks. The experimental orientations of the solutes dissolved in ZLI1132, EBBA, and the magic mixture are presented together with the simulated points that were obtained by choosing ϵ values that generate physically sensible calculated data. (Regarding the calculated data, notice that our procedure is not a fitting in the strict sense of the word because there is not an algorithm aiming to minimize the rms between experimental and calculated dipolar couplings by properly changing some adjustable parameter.) The matching of simulated data with the solute order parameters in the magic mixture is really excellent: often, the overlapping is so strong that the simulated points eclipse the experimental ones. On the contrary, the behaviors in the other nematic solvents, where additional interactions are thought to play a significant role, are not reproduced at all by this purely short-range anisotropic potential. Regarding this, it should be remembered that PBZQ, DNOB, and DCNB have strong local dipoles[32] (−CO = 7.66; −CN = 13.0; $-NO_2$ = 13.2; all values are given in C m × 10^{30}). In the past, the effects of the electric dipoles of the bonds were investigated as a possible cause of ordering, but different authors came to discordant conclusions: some studies[33−35] claimed the importance of dipoles as orientational mechanisms whereas other works stated their negligibility.[36,37] Our very good results, obtained with a potential that does not take into account dipolar interactions, seem to confirm that local dipoles, at least

TABLE 4: Experimental Dipolar Couplings from ^{1}H NMR Spectra of Biphenylene Dissolved in Nematic Solvents ZLI1132 and EBBA and the 55 wt % ZLI1132 + EBBA Magic Mixture at Different Temperatures

	ZLI1132	EBBA	ZLI + EBBA
T/K	294	294	294
D_{12}[a]	−1949.92 ± 0.03	−1791.39 ± 0.03	−1776.56 ± 0.03
D_{13}	−124.22 ± 0.05	−16.91 ± 0.04	−86.05 ± 0.08
D_{14}	4.60 ± 0.16	94.87 ± 0.08	28.80 ± 0.23
D_{15}	−60.01 ± 0.16	−32.53 ± 0.10	−48.83 ± 0.25
D_{16}	−87.82 ± 0.06	−79.77 ± 0.05	−79.72 ± 0.08
D_{17}	−179.12 ± 0.04	−180.31 ± 0.04	−167.44 ± 0.07
D_{18}	−751.88 ± 0.11	−768.09 ± 0.09	−706.38 ± 0.18
D_{23}	60.23 ± 0.16	851.34 ± 0.09	274.43 ± 0.24
D_{26}	−65.44 ± 0.17	−64.94 ± 0.09	−60.70 ± 0.26
D_{27}	−81.02 ± 0.12	−82.41 ± 0.10	−76.25 ± 0.20
T/K	298	298	298
D_{12}	−1890.20 ± 0.07	−1771.70 ± 0.04	−1733.53 ± 0.06
D_{13}	−123.71 ± 0.09	−17.91 ± 0.05	−86.02 ± 0.07
D_{14}	−0.09 ± 0.28	92.68 ± 0.07	27.08 ± 0.24
D_{15}	−58.73 ± 0.29	−32.48 ± 0.10	−48.48 ± 0.23
D_{16}	−85.16 ± 0.08	−79.09 ± 0.06	−77.88 ± 0.09
D_{17}	−172.91 ± 0.07	−178.06 ± 0.05	−163.35 ± 0.07
D_{18}	−725.89 ± 0.16	−758.73 ± 0.10	−687.44 ± 0.20
D_{23}	25.71 ± 0.29	832.81 ± 0.07	251.98 ± 0.26
D_{26}	−63.38 ± 0.28	−64.21 ± 0.10	−58.28 ± 0.23
D_{27}	−78.50 ± 0.18	−81.51 ± 0.11	−74.44 ± 0.22
T/K	301	303	303
D_{12}	−1838.78 ± 0.06	−1724.11 ± 0.04	−1660.55 ± 0.09
D_{13}	−123.91 ± 0.13	−19.94 ± 0.06	−85.26 ± 0.11
D_{14}	−2.46 ± 0.31	87.83 ± 0.11	23.39 ± 0.37
D_{15}	−59.25 ± 0.33	−32.06 ± 0.12	−46.83 ± 0.35
D_{16}	−83.04 ± 0.13	−76.95 ± 0.06	−74.69 ± 0.11
D_{17}	−167.30 ± 0.09	−172.89 ± 0.06	−155.82 ± 0.10
D_{18}	−703.67 ± 0.20	−736.54 ± 0.11	−656.96 ± 0.26
D_{23}	−2.35 ± 0.33	788.61 ± 0.11	216.94 ± 0.37
D_{26}	−60.83 ± 0.35	−62.32 ± 0.11	−56.07 ± 0.32
D_{27}	−76.20 ± 0.23	−78.78 ± 0.12	−70.43 ± 0.29
T/K	309	307	308
D_{12}	−1771.65 ± 0.11	−1639.12 ± 0.04	−1577.41 ± 0.14
D_{13}	−122.30 ± 0.20	−23.26 ± 0.06	−84.02 ± 0.18
D_{14}	−8.67 ± 0.68	79.52 ± 0.11	17.30 ± 0.52
D_{15}	−54.85 ± 0.75	−31.56 ± 0.13	−47.05 ± 0.60
D_{16}	−81.23 ± 0.21	−73.21 ± 0.07	−70.63 ± 0.20
D_{17}	−161.06 ± 0.13	−163.69 ± 0.06	−147.14 ± 0.17
D_{18}	−675.00 ± 0.35	−696.58 ± 0.12	−622.24 ± 0.43
D_{23}	−29.09 ± 0.67	713.69 ± 0.12	183.30 ± 0.54
D_{26}	−63.06 ± 0.76	−59.45 ± 0.12	−52.78 ± 0.54
D_{27}	−72.21 ± 0.39	−74.93 ± 0.13	−66.39 ± 0.47
T/K	315	317	313
D_{12}	−1698.67 ± 0.06	−1547.84 ± 0.07	−1491.43 ± 0.11
D_{13}	−122.19 ± 0.12	−26.14 ± 0.09	−82.14 ± 0.15
D_{14}	−9.57 ± 0.41	71.29 ± 0.18	16.25 ± 0.46
D_{15}	−56.69 ± 0.39	−30.15 ± 0.18	−42.05 ± 0.44
D_{16}	−76.53 ± 0.13	−69.30 ± 0.11	−66.92 ± 0.16
D_{17}	−153.62 ± 0.08	−153.86 ± 0.10	−139.04 ± 0.13
D_{18}	−644.46 ± 0.22	−654.77 ± 0.19	−587.04 ± 0.35
D_{23}	−64.99 ± 0.44	638.94 ± 0.19	147.67 ± 0.48
D_{26}	−56.27 ± 0.41	−56.08 ± 0.20	−52.02 ± 0.46
D_{27}	−69.21 ± 0.27	−69.93 ± 0.20	−61.61 ± 0.38

[a] Because of the D_{2h} molecular symmetry of BPLN, the following relations hold: $D_{12} = D_{34} = D_{56} = D_{78}$; $D_{17} = D_{28} = D_{35} = D_{46}$; $D_{27} = D_{36}$; $D_{26} = D_{37}$; $D_{16} = D_{25} = D_{38} = D_{47}$; $D_{13} = D_{24} = D_{57} = D_{68}$; $D_{23} = D_{67}$; $D_{18} = D_{45}$; $D_{15} = D_{48}$; $D_{14} = D_{58}$.

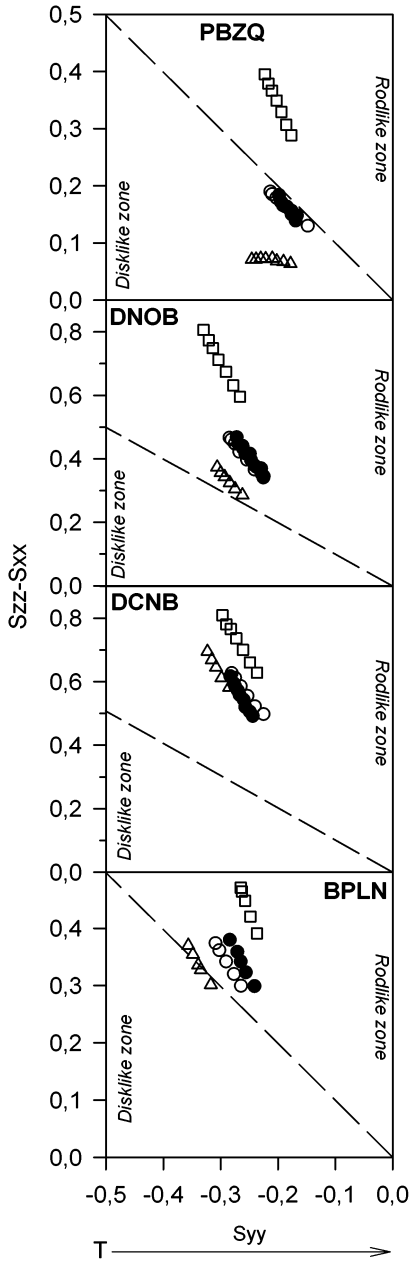

Figure 3. Simulated (●) and experimental $\mathbf{S}_{zz}-\mathbf{S}_{xx}$ vs $\mathbf{S}_{yy}$ for *p*-benzoquinone, 1,4-dinitrobenzene, 1,4-dicyanobenzene, and biphenylene (from top to bottom) dissolved in ZLI1132 (△), EBBA (□), and the 55 wt % ZLI1132 + EBBA magic mixture (○).

TABLE 5: Dimensions of *p*-Benzoquinone (PBZQ), 1,4-Dinitrobenzene (DNOB), 1,4-Dicyanobenzene (DCNB), and Biphenylene (BPLN)

	PBZQ	DNOB	DCNB	BPLN
L/Å	8.21	9.85	11.50	10.35
W/Å	6.66	6.70	6.70	7.70
B/Å	3.40	3.40	3.80	3.40

in the magic mixture, do not produce appreciable effects on the orientation.

Regarding DNOB, the good outcome obtained in reproducing its order parameters could be considered to be an indirect validation of the conformation assumed for the calculations, so from this evidence, we can infer that DNOB, at least in the magic mixture, exhibits a conformation that is similar to that in the crystal, where the nitro groups are twisted not more than about 10°.

The data of BPLN appear to be slightly shifted with respect to the that of the experiments (see Figure 3, bottom), but our choice of geometries and, especially, of vdW radii was as unbiased as possible in order to test the real efficiency of the model: it is possible to reproduce the experiments perfectly by increasing the *W*/*L* ratio of the BPLN box by a very small amount (∼2%).

To summarize the results presented thus far, it can be said that they corroborate results that were previously obtained by simulation techniques[38,39] and strengthen the common approximation that it is possible to neglect long-range effects in very dilute magic mixture solutions where large biaxial molecules are dissolved without significant consequences on the prediction of order parameters; at the same time, these outcomes support, by a synergistic effect, the reliability of the suggested short-range potential.

It is interesting to point out the large spreading of the orientational behaviors of PBZQ as the nematic solvent is changed (see Figure 3, top): from disk, in ZLI1132, to rod, in EBBA. (In our picture, the difference between a disk and a rod depends on the sign of $\mathbf{S}_{xx}$: $\mathbf{S}_{xx} > 0$ = disk; $\mathbf{S}_{xx} < 0$ = rod.) This is, to our knowledge, the second time that this effect is observed: only 1,4-difluorobenzene (DFB; see Figure 1, top, in ref 11) showed this behavior before. The nature of this phenomenon should be mainly attributed to long-range interactions because the behavior in the magic mixture (free from long-range effects) is in the middle between the rod and disk. Nevertheless, it arises only when, as for DFB and PBZQ, the solute does not have a marked rod or disk shape. In other cases, where the solute shapes are strongly characterized as, for example, rods (1,4-dichlorobenzene and 1,4-dibromobenzene in ref 11; 1,4-dinitrobenzene and 1,4-dicyanobenzene in this work), the ordering, even though it changes with solvent for all of the solutes studied, is basically imposed by the shape, and such a large spreading does not occur despite the presence of strong local dipoles or quadrupolar effects. This can be considered further proof that, as pointed out in the Introduction, the size and shape mechanism can actually be recognized as having the leading (but not the absolute) role in the solute ordering; only when the solute shape is not markedly defined do long-range effects become discriminating.

Magic Solutes. The very good results obtained in the past[11] (and in this study for PBZQ, DNOB, DCNB, and BPLN) encouraged us to test our model on the so-called magic solutes, which are relatively inert molecules whose shape-dominated ordering in nematic solvents is reported in the literature.[3] In ref 3, cycloalkane solutes dissolved in ZLI2452 (a mixture of mesogens including cyano- and alkyl-substituted phenylcyclohexanes and biphenylcyclohexanes, alkylcyclohexylbiphenylcyclohexanes, and cyclohexyl carbonates by Merck, Ltd.) have been studied by deuterium NMR. ZLI2452 exhibits one of the widest known nematic ranges (120 °C), so orientational data can be studied over a very large range of temperature (from −40 to 80 °C). Using the data of ref 3, we tested our method on the most symmetric molecules treated in that work: D_{3d} cyclohexane (CYHX) and C_{2h} 1,4-*trans*-dimethylcyclohexane (*t*-DMCH) and *trans*-decalin (*t*-DCLN). (The structures and the molecular reference systems chosen according to ref 3 are reported in Figure 4.) We assumed for the solutes the geometries given in Table 2 of ref 3 rotated about the *z* axis by 19° and 17° for 1,4-*trans*-dimethylcyclohexane and *trans*-decalin, respectively (as indicated in the cited paper), in order to work in the **S**-matrix principal axis system. The vdW radii of H and C have been taken from ref 26, but the methyl group in *t*-DMCH

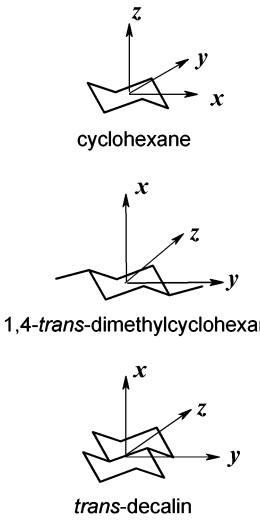

Figure 4. Structures and reference systems of magic solutes.

TABLE 6: Dimensions of Cyclohexane (CYHX), 1,4-*trans*-Dimethylcyclohexane (*t*-DMCH), and *trans*-Decalin (*t*-DCLN)

	CYHX	*t*-DMCH	*t*-DCLN
L/Å	5.25	6.74	9.28
W/Å	7.04	5.12	5.17
B/Å	7.04	9.85	7.40

has been considered as a whole, with a vdW radius of 2.2 Å as reported in ref 28. The molecules were boxed in hard parallelepipeds with the faces parallel to the (*xy*), (*xz*), and (*yz*) planes, and the *L*, *W*, and *B* values, given in Table 6, were taken along *z*, *x*, and *y* axes, respectively, by analogy to the choice made for the solutes that were previously treated. Two clarifications have to be made at this point: (1) Because of its high symmetry, needing just one order parameter, the relation $W = B = (W + B)/2$ has been set for CYHX. (2) The investigated temperatures also involve the range where CYHX and *t*-DMCH interconvert between their chair conformations (being much higher in energy, the boat structures can be safely neglected). The two chair forms of each molecule have identical geometries, and hence they fit into the same box, so the dimensions of the boxes (Table 6) are in practice not affected by the interconversion. In Figure 5, the experimental data $\mathbf{S}_{xx}$, $\mathbf{S}_{yy}$, and $\mathbf{S}_{zz}$ taken from ref 3 are compared with the simulated points $\mathbf{S}_{xx}$, $\mathbf{S}_{yy}$, and $\mathbf{S}_{zz}$ for CYHX (top), *t*-DMCH (middle), and *t*-DCLN (bottom). The orientational behavior of each solute in ZLI2452 is very well reproduced over the entire range of temperature. (The imperfect fit of the only order parameter of CYHX can be easily justified since, as stated above, our procedure is not a fitting and ϵ is not an ad hoc adjustable parameter.) The good results obtained for magic solutes represent once more, in our opinion, incontrovertible proof that our model is really able to describe in an exhaustive way short-range orientational interactions.

In Figure 6, the symbols plotted versus *T* represent the ϵ values producing the calculated order parameters shown in Figures 3 and 5. In principle, the ϵ parameter should be identical for all solutes in the same solvent at the same temperature, but it is not surprising, in so a simple and schematic (but effective) description of the orientational phenomenon, that the ϵ values deviate from ideal behavior. We think that in this case arguments similar to those given by Terzis et al.,[3] in a different context, about their *p* parameter can be used; in particular, the neglect of correlations among the solvent molecules could be responsible for the observed solute dependence of ϵ. Moreover, in the range of studied temperatures, a roughly linear dependence of ϵ on *T*

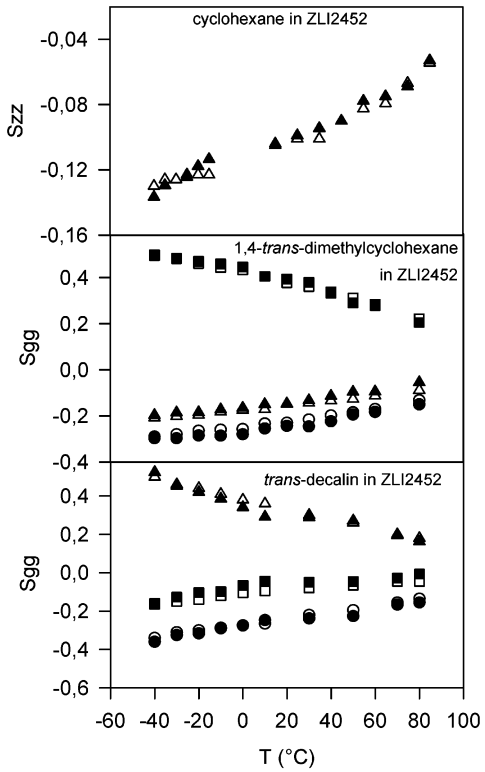

Figure 5. Simulated (full symbols) and experimental (open symbols) $\mathbf{S}_{zz}$ (triangles), $\mathbf{S}_{xx}$ (circles), and $\mathbf{S}_{yy}$ (squares) for magic solutes cyclohexane, 1,4-*trans*-dimethylcyclohexane, and *trans*-decalin in ZLI2452 (from the top). Experimental values are taken from ref 3.

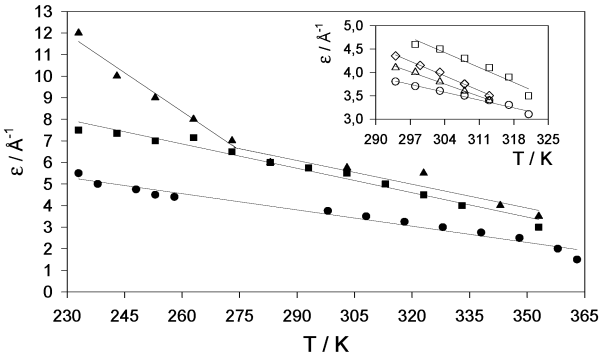

Figure 6. Plots of ϵ vs *T* for *trans*-decalin (▲), 1,4-*trans*-dimethylcyclohexane (■), cyclohexane (●) and (inset) *p*-benzoquinone (○), 1,4-dinitrobenzene (□), 1,4-dicyanobenzene (△), and biphenylene (◇). The straight lines result from linear fittings of the points.

can be recognized (the solid lines in Figure 6 are obtained by linear fittings of the points), except for *t*-DCLN, where two slopes are present (from 230 to 290 K and from 290 to 350 K). The study of this behavior, which is beyond the scope of this paper, is planned for the future, and at the moment, an interpretation would be too pretentious. For now, we prefer to give this as an empirical statement of the facts.

Conclusions

Some final remarks about the work presented above can be made. The proposed model proved to be a highly reliable and very effective tool for the description of orientational order when short-range interactions totally control the solute ordering. In light of the obtained results, the simplicity of the adopted model should be considered to be advantage rather than a limitation since the basic orientational information produced by this

essential treatment agrees very well with NMR experimental data. However, the argument can be reversed: the fact that such a strictly short-range potential, where only a coarse description of the solute and solvent is given, is able to reproduce very well the order parameters of apolar solutes in the 55 wt % ZLI1132+EBBA magic mixture (but not in other solvents) and of magic solutes in a generic nematic solvent should be taken as further proof that solely short-range orientational mechanisms are decisive in those situations. The two points of view are not competitive, but rather they strengthen each other by synergy: this fact emphasizes even more, in our opinion, the validity of the proposed approach. The development of the work will reckon with the extension of the model to the description of long-range mechanisms (mainly the solute electric quadrupole−solvent electric field gradient interaction). In particular, we would like to be able to predict the very peculiar orientational behaviors of *p*-benzoquinone and 1,4-difluorobenzene[11] from disk to rod as the solvent is changed.

Acknowledgment. This work has been supported by MIUR PRIN ex 40%. We thank Professor M. Longeri (Dipartimento di Chimica−Università della Calabria) for the critical reading of the manuscript.

References and Notes

(1) Saupe, A.; Englert G. *Phys. Rev. Lett.* **1963**, *11*, 462.
(2) Emsley, J. W., Ed. *Nuclear Magnetic Resonance of Liquid Crystals*; Reidel: Dordrecht, The Netherlands, 1985.
(3) Terzis, A. F.; Poon, C.-D.; Samulski, E. T.; Luz, Z.; Poupko, R.; Zimmermann, H.; Müller, K.; Toriumi, H.; Photinos, D. J. *J. Am. Chem. Soc.* **1996**, *118*, 2226 and references therein.
(4) Burnell, E. E.; de Lange, C. A. *Chem. Rev.* **1998**, *98*, 2359 and references therein.
(5) Williams, V. E.; Lemieux, R. P. *J. Am. Chem. Soc.* **1998**, *120*, 11311.
(6) di Matteo, A.; Ferrarini, A.; Moro, G. J. *J. Phys. Chem. B* **2000**, *104*, 7764.
(7) di Matteo, A.; Ferrarini, A. *J. Phys. Chem. B* **2001**, *105*, 2837.
(8) Celebre, G.; De Luca, G.; Ferrarini, A. *Mol. Phys.* **1997**, *92*, 1039 and references therein.
(9) Barker, P. B.; Van der Est, A. J.; Burnell, E. E.; Patey, G. N.; de Lange, C. A.; Snijders, J. G. *Chem. Phys. Lett.* **1984**, *107*, 426.
(10) Celebre, G. *Chem. Phys. Lett.* **2001**, *342*, 375.
(11) Celebre, G. *J. Chem. Phys.* **2001**, *115*, 9552.
(12) Fabbri, U.; Zannoni, C. *Mol. Phys.* **1983**, *49*, 1321.
(13) (a) Allen, M. P.; Tildesley, D. J. *Computer Simulation of Liquids*; Clarendon: Oxford, U.K., 1987. (b) Metropolis, N.; Rosenbluth, A. W.; Rosenbluth, M. N.; Teller, A. H.; Teller, E. *J. Chem. Phys.* **1953**, *21*, 1087.
(14) Straley, J. P. *Phys. Rev. A: At., Mol., Opt. Phys.* **1974**, *10*, 1881.
(15) Hashim, R.; Luckhurst, G. R.; Romano, S. *Mol. Phys.* **1985**, *56*, 1217.
(16) Zannoni, C. In *The Molecular Physics of Liquid Crystals*; Luckhurst, G. R., Gray, G. W., Eds.; Academic Press: London, 1979; Chapter 9.
(17) (a) Vogel, A. I. *Vogel's Textbook of Practical Organic Chemistry*, 5th ed.; Longman Scientific & Technical: Harlow, England, 1989. (b) March, J. *Advanced Organic Chemistry*; Wiley: New York, 1992.
(18) (a) Stephenson, D. S.; Binsch, G. *J. Magn. Reson.* **1980**, *37*, 395. (b) Stephenson, D. S.; Binsch, G. *Org. Magn. Reson.* **1980**, *14*, 226. (c) Stephenson, D. S.; Binsch, G. *Mol. Phys.* **1981**, *43*, 697.
(19) Castiglione, F.; Carravetta, M.; Celebre, G.; Longeri, M. *J. Magn. Reson.* **1998**, *132*, 1.
(20) Celebre, G.; De Luca, G.; Longeri, M.; Sicilia, E. *J. Chem. Inf. Comput. Sci.* **1994**, *83*, 309.
(21) Castellano, S.; Bothner-By, A. A. *J. Chem. Phys.* **1964**, *41*, 3863.
(22) Polson, J. M.; Burnell, E. E. *J. Magn. Reson., Ser. A* **1994**, *106*, 223.
(23) Nonella, M.; Tavan, P. *Chem. Phys.* **1995**, *199*, 19.
(24) Ivanov, P. M. *J. Mol. Struct.* **1998**, *440*, 237.
(25) Andreev, G. N.; Stamboliyska, B. A.; Penchev, P. P. *Spectrochim. Acta, Part A* **1997**, *53*, 811.
(26) Bondi, A. *J. Phys. Chem.* **1964**, *68*, 441.
(27) Rowland, R. S.; Taylor, R. *J. Phys. Chem.* **1996**, *100*, 7384.
(28) Badenhoop, J. K.; Weinhold, F. *J. Chem. Phys.* **1997**, *107*, 5422.
(29) Batsanov, S. S. *Struct. Chem.* **2000**, *11*, 177.
(30) Trotter, J. *Can. J. Chem.* **1961**, *39*, 1638.
(31) Tonogaki, M.; Kawata, T.; Ohba, S.; Iwata, Y.; Shibuya, I. *Acta Crystallogr., Sect. B* **1993**, *49*, 1031.
(32) Chelkowski, A. *Dielectric Physics*; Elsevier: Amsterdam, 1980.
(33) Photinos, D. J.; Poon, C.-D.; Samulski, E. T.; Toriumi, H. *J. Phys. Chem.* **1992**, *96*, 8176.
(34) Photinos, D. J.; Samulski, E. T. *J. Chem. Phys.* **1993**, *98*, 10009.
(35) Terzis, A. F.; Photinos, D. J. *Mol. Phys.* **1994**, *83*, 847.
(36) Syvitski, R. T.; Burnell, E. E. *Chem. Phys. Lett.* **1997**, *281*, 199.
(37) Syvitski, R. T.; Burnell, E. E. *J. Chem. Phys.* **2000**, *113*, 3452.
(38) Polson, J. M.; Burnell, E. E. *Mol. Phys.* **1996**, *88*, 767.
(39) Syvitski, R. T.; Polson, J. M.; Burnell, E. E. *Int. J. Mod. Phys. C* **1999**, *10*, 403.